

SOLVENT-KAOLINITE INTERACTIONS INVESTIGATED USING THE 3D-RISM-KH MOLECULAR THEORY OF SOLVATION

STANISLAV R. STOYANOV^{1,2,*}, FENG LIN¹, AND YUMING XU¹

¹ Natural Resources Canada, CanmetENERGY in Devon, 1 Oil Patch Drive, Devon, AB T9G 1A8, Canada

² Department of Chemical and Materials Engineering, University of Alberta, 9211 116 Street NW, Edmonton, AB T6G 1H9, Canada

Abstract—The oil sands of western Canada represent the third largest hydrocarbon deposit in the world. Bitumen, a very heavy petroleum, is recovered from mined oil sands using warm water extraction followed by separation treatments to isolate the bitumen product. The high energy, water use, as well as tailings remediation challenges associated with the warm water extraction process raise major environmental concerns. Non-aqueous extraction using organic solvents at room temperature has been investigated extensively as an alternative to the warm water extraction process. The main challenge to the large-scale implementation of non-aqueous extraction is the retention of solvent in the tailings. The objective of this work was to present and validate a computational model for the interaction of solvents used in non-aqueous extraction with minerals, such as the abundant and adsorbent clay mineral kaolinite. The model system contained a periodically extended kaolinite platelet immersed in a solvent and all were treated at the atomic level using the 3D Reference Interaction Site Model with the Kovalenko-Hirata closure approximation (3D-RISM-KH) molecular theory of solvation. The solvent solvation free energy of interaction with kaolinite as well as site-specific adsorption energies and kinetic barriers for desorption were computed based on the solvent site density distribution functions. Moreover, the lateral and integrated density distributions were computed to analyze the organization of solvent at kaolinite surfaces. The integrated density distribution profiles were correlated with experimental adsorption isotherms. The results showed very strong adsorption of ethanol and weak adsorption of hydrocarbon solvents on kaolinite, which were in qualitative agreement with experimental solvent extraction reports. The model and these findings are valuable in understanding the mechanism of solvent retention in tailings after non-aqueous extraction and highlight the action of hydroxylated cosolvent additives to enhance extraction using nonpolar solvents.

Key Words—Adsorption Energy, Density Distribution Function, Kaolinite, Kinetic Barrier For Desorption, Non-aqueous Extraction, Oil Sands Bitumen, Solvent Retention, Tailings.

INTRODUCTION

The currently used warm water process for extraction of bitumen from oil sands includes oil sand slurry preparation, aeration, separation of the floating bitumen-rich froth, and treatment of the bitumen froth using a light hydrocarbon solvent to separate water and mineral solids from the bitumen product. While a large part of the water used in extraction is recycled, about 1 m³ of water per barrel of the crude bitumen produced is trapped in a stable suspension known as a mature fine tailings (MFT) that takes anywhere from a few decades to a few hundred years to ultimately consolidate (Eckert *et al.*, 1996; Masliyah *et al.*, 2011). The increasing volumes of MFT that have been produced create significant operational and environmental challenges.

An important alternative to warm water extraction is the use of non-aqueous media, typically hydrocarbon solvents at room temperature in an approach known as

non-aqueous extraction. The obvious benefits of non-aqueous extraction are the decreased water use or no water use, a smaller amount of tailings, and the anticipated lower energy use due to the lower extraction temperature. Moreover, non-aqueous extraction processes are effective for the extraction of bitumen from low-quality ores, which are defined as containing less than 8% bitumen based on the recovery limit of the warm water extraction process, as well as ores that have high contents of sand and clay fines (Lin *et al.*, 2017). Economic recovery from low-quality deposits helps convert in-place resources to established reserves. The non-aqueous extraction processes also produce bitumen with a low fines content due to the limited release of fines and the more effective separation of bitumen from fines (Lin *et al.*, 2017).

Despite its apparent environmental, energy, and water use advantages, as well as the large number of patents and extensive research in the last 50 years, non-aqueous extraction technology has not yet been implemented for bitumen extraction from oil sands on a large scale. The reasons for this can be attributed to the challenges faced by non-aqueous extraction process developers, as discussed in a recent review (Lin *et al.*, 2017). Unlike water tailings, the organic solvent-wetted tailings from

* E-mail address of corresponding author:

stanislav.stoyanov@canada.ca

DOI: 10.1346/CCMN.2018.064098

© Her Majesty the Queen in Right of Canada, as represented by the Minister of Natural Resources, 2018

non-aqueous extraction cannot be released to the environment because the solvents are generally harmful to wildlife, vegetation, and human health. The Alberta Energy Regulator has set a limit of 4 volumes of light hydrocarbon solvent lost (mainly from bitumen froth treatment) per 1000 volumes of bitumen product for the existing water-based technology and companies have achieved sustained loss rates as low as $3 \text{ m}^3/1000 \text{ m}^3$ (Nikakhtari *et al.*, 2013). On this basis, a residual solvent concentration of 260 mg/kg in the tailings (water-free basis) would exceed the current industry performance (Nikakhtari *et al.*, 2013). In any viable non-aqueous extraction process, a solvent removal step has to be included to recover the solvent from the solids.

In recent studies, solvent recovery and residual solvent concentrations in the tailings produced are among the criteria for ranking extraction solvents, along with bitumen recovery and solids content in the bitumen product (Painter *et al.*, 2010; Li *et al.*, 2012; Wu and Dabros, 2012; Wang *et al.*, 2014; Osacky *et al.*, 2015; Pal *et al.*, 2015; Nikakhtari *et al.*, 2013, 2016). These non-aqueous extraction studies show that cyclic aliphatic hydrocarbon solvents, such as cyclopentane and cyclohexane, achieve good performance for bitumen recovery, fines rejection, and residual bitumen concentrations in tailings (Wu and Dabros, 2012; Nikakhtari *et al.*, 2013). Other advantages of cyclic aliphatic solvents are relatively low toxicity, odor, and boiling points (Wu and Dabros, 2012; Pal *et al.*, 2015). In the Nikakhtari *et al.* (2013) study, aromatics, cycloalkanes, biologically derived solvents, and mixtures of solvents were evaluated with respect to the performance of the non-aqueous extraction process. The residual solvent concentrations after the secondary tailings were dried were linearly correlated to the solvent vapor pressures, except for isoprene, which has a very high vapor pressure and a very low residual content, as well as cyclohexane, which has a very low residual content (Nikakhtari *et al.*, 2013).

The influence of non-swelling clay minerals on non-aqueous fluid extraction of bitumen from oil sands was investigated using artificial mixtures of bitumen that contained natural kaolinite, illite, and chlorite clay standards (Osacky *et al.*, 2015). The results showed that the total measured amounts of residual cyclohexane-insoluble organic carbon in clay-bitumen mixtures after non-aqueous bitumen extraction was dependent on both the intrinsic resistance of organic macromolecules to cyclohexane extraction and the nature of the non-swelling clays. The non-swelling clays retained cyclohexane-insoluble organic carbon mainly on clay particle edges and basal planes in patches rather than continuous coatings according to X-ray diffraction analysis results (Osacky *et al.*, 2015).

Recently, the sorption and desorption kinetics of cyclohexane, toluene, and water to kaolinite, fine solids, and organic-rich fine solids that were isolated from Athabasca oil sands were gravimetrically measured and

reported for a range of solvent vapor concentrations. The solvent sorption mechanism depended on the particle size, the organic material content, and the organic material distribution on particle surfaces. The adsorption decreased as specific interactions decreased in the order water > toluene > cyclohexane because water forms strong hydrogen bonds with kaolinite and toluene interacts with kaolinite through weaker interactions between toluene π -electrons and kaolinite surface hydroxyl groups. Saturated hydrocarbons only interact with solids *via* weak van der Waals forces (Tan *et al.*, 2016).

Kaolinite is a 1:1 phyllosilicate that is composed of octahedral AlOH sheets coupled with tetrahedral SiO sheets (Bish and Johnston, 1993; Cygan *et al.*, 2004). Kaolinite layers stack together and are stabilized by a network of hydrogen bonds between the hydroxyl groups and the SiO surface (Allen and Hajek, 1989; Painter *et al.*, 2010). The high abundance of fines in the Athabasca oil sands is considered a major challenge to bitumen recovery (Bensebaa *et al.*, 2000; Sparks *et al.*, 2003; Osacky *et al.*, 2015; Lin *et al.*, 2017).

Kaolinite interactions with organic molecules have been investigated computationally using atomic molecular simulations and implicit methods. Studies of the competitive adsorption of pyridine, heptane, and water on kaolinite using molecular dynamics show stronger bonding of polar molecules to kaolinite AlOH surfaces (Ni and Choi, 2012). The adsorption of polar, non-polar, and amphiphilic molecules to kaolinite has also been investigated using molecular dynamics to determine the surface adsorption preferences (Underwood *et al.*, 2016). Monte Carlo simulations of the intercalation of small organic molecules into kaolinite suggest multiple system states coexist (Rutkai and Kristof, 2008). An implicit solvent method based on a density functional that was inferred from bulk solvent properties has been employed to study clay surface solvation (Levesque *et al.*, 2012). Important to note is that lengthy molecular simulations are required to obtain the statistical sampling necessary to adequately address solvation thermodynamics. In this respect, implicit methods could help to decrease the computing cost.

An advanced computational method to model solvation thermodynamics, the three-dimensional reference interaction site model theory using the closure approximation of Kovalenko and Hirata (2000) (3D-RISM-KH), has been successfully employed to understand a wide range of processes and interactions at interfaces and in supramolecular systems (Kovalenko and Hirata, 2000a and 2000b; Kovalenko, 2003). Based on the fundamental Ornstein-Zernike equation for a bulk molecular fluid, the 3D-RISM site approach implies that the orientations of the site correlation functions are averaged (Kovalenko, 2003; Hansen and McDonald, 2006). Also important to note is that closure relations, such as KH, introduce approximations in the solvation free energy calculations that are corrected using linear functions (Palmer *et al.*, 2010; Huang *et al.*, 2015). The

3D-RISM-KH molecular theory of solvation properly accounts for hydrophobic and hydrogen bonding interactions and reproduces structural and phase transitions in simple and complex liquids over a wide range of thermodynamic conditions (Kovalenko and Hirata, 2001; Yoshida *et al.*, 2002) and accounts for nanoporous confinement (Tanimura *et al.*, 2007). The 3D-RISM-KH theory has been employed to predict the solvation structure and thermodynamics of gelation activity (Kovalenko *et al.*, 2012); molecular boundary conditions of hydrodynamic flow (Kobryn and Kovalenko, 2008); self-assembly of rosette nanotubes (Moralez *et al.*, 2005); molecular recognition in biomolecular nanosystems (Yamazaki *et al.*, 2008); nanoscale forces in plant cell walls (Silveira *et al.*, 2013, 2015); and hydrothermal pretreatment of cellulosic biomass (Silveira *et al.*, 2016).

In heavy oil research, the aggregation of petroleum asphaltene in quinoline and 1-methylnaphthalene solvents at elevated temperature (Stoyanov *et al.*, 2008) and thiophenic heterocycle adsorption to ion-exchanged zeolite surfaces in benzene have been studied using the 3D-RISM-KH theory (Stoyanov *et al.*, 2011). The effect of trace amounts of water in chloroform on the free energy of asphaltene model compound aggregation was investigated using the 3D-RISM-KH theory and the contributions of hydrogen bonding and π - π stacking interactions to aggregation were evaluated based on electronic structure calculations (Costa *et al.*, 2012a, 2012b). The results have been correlated with the experimental ^1H NMR chemical shifts indicative of aggregation (Tan *et al.*, 2009).

The 3D-RISM-KH method has been employed to study the interactions between organic molecules and kaolinite suspensions as model systems for oil sands. A study of indole adsorption to kaolinite presented insights into the preferred adsorption orientation and the potential for effective indole adsorption from heptane and toluene solvents. Calculated multilayer adsorption profiles were correlated with experimentally determined monolayer and saturation organoclay loading driven by strong adsorbate-adsorbate interactions (Fafard *et al.*, 2013). The molecular recognition interactions of S- and N-containing heterocycles with kaolinite were investigated in toluene using the 3D-RISM-KH method to gain insights into this entropy-driven organization, and were correlated with experimental adsorption kinetics and thermodynamics studies (Huang *et al.*, 2014). Adsorption isotherms of heterocyclic compounds over a range of extraction temperatures in toluene and in cyclohexane solvents were computed using the solvent site distribution functions (Hlushak and Kovalenko, 2017). Selective bitumen extraction and removal from oil sands using liquid and supercritical CO_2 was modeled

to evaluate the performance of this underutilized extraction solvent (Lage *et al.*, 2015). The mechanism of action of flocculant additives for the enhanced aggregation of kaolinite platelets in aqueous electrolyte solutions was also investigated (Hlushak *et al.*, 2016).

The purpose of the present work was to present an atomic-level model of solvated kaolinite that allows the calculation of solvent retention and release thermodynamics and kinetics, and to evaluate the performance of the model for aliphatic, aromatic, and polar solvents by comparing results with experimental findings.

MATERIALS AND METHODS

Computational modeling technique

Overview of 3D-RISM-KH theory. The 3D-RISM-KH molecular theory of solvation couples the 3D-RISM integral equation 1 for 3D solute-solvent site correlation functions (Chandler *et al.*, 1986a, 1986b) with the 3D Kovalenko-Hirata (KH) closure approximation (equation 2), as follows:

$$h_\gamma(\mathbf{r}) = \sum_\alpha \int d\mathbf{r}' c_\alpha(\mathbf{r} - \mathbf{r}') \chi_{\alpha\gamma}(r') \quad (1)$$

$$h_\gamma(\mathbf{r}) = \begin{cases} \exp(d_\gamma(\mathbf{r})) - 1 & \text{for } d_\gamma(\mathbf{r}) \leq 0 \\ d_\gamma(\mathbf{r}) & \text{for } d_\gamma(\mathbf{r}) > 0 \end{cases}$$

$$d_\gamma(\mathbf{r}) = -\mu_\gamma(\mathbf{r})/(k_B T) + h_\gamma(\mathbf{r}) - c_\gamma(\mathbf{r}) \quad (2)$$

where $h_\gamma(\mathbf{r})$ and $c_\gamma(\mathbf{r})$ are the 3D total and direct correlation functions, respectively, of the solvent site γ around the solute, $\chi_{\alpha\gamma}(\mathbf{r})$ is the site-site susceptibility of the solvent which is calculated beforehand, and the α and γ indices enumerate all the interaction sites on all sorts of solvent species. The 3D distribution function $g_\gamma(\mathbf{r})$ of solvent site γ is related to $h_\gamma(\mathbf{r})$ as $g_\gamma(\mathbf{r}) = h_\gamma(\mathbf{r}) + 1$. A $g_\gamma(\mathbf{r})$ value of 1.0 corresponds to a bulk solvent distribution far from the solute. When $g_\gamma(\mathbf{r}) > 1.0$, the solvent site density is greater than the bulk solvent. When $g_\gamma(\mathbf{r}) < 1.0$, the solvent density is less than the bulk solvent. The 3D interaction potential $u_\gamma(\mathbf{r})$ between the whole solute and solvent site γ is specified by a molecular force field and $k_B T$ is the Boltzmann constant times the solution temperature. Equations 1 and 2 are forced to converge to a relative root mean square accuracy of 10^{-4} by using the modified direct inversion in the iterative subspace (MDIIS) of the accelerated numerical solver for integral equations in liquid state theory (Kovalenko and Hirata, 2000a, 2000b; Kovalenko, 2003).

The solvation free energy $\mu_{\text{solv}}^{\text{KH}}$ of a solute in a solvent that follows from the 3D-RISM-KH equations 1 and 2 is given by the closed analytical equation 3 (Kovalenko and Hirata, 2000a, 2000b)

$$\mu_{\text{solv}}^{\text{KH}} = k_B T \sum_\gamma \rho_\gamma \int d\mathbf{r} \left[\frac{1}{2} h_\gamma^2(\mathbf{r}) \Theta(-h_\gamma(\mathbf{r})) - c_\gamma(\mathbf{r}) - \frac{1}{2} h_\gamma(\mathbf{r}) c_\gamma(\mathbf{r}) \right] \quad (3)$$

where the sum enumerates all of the solvent species sites and Θ is the Heaviside unit step function (Heaviside 1885, 1886, 1887).

The strength with which a solvent site interacts with a solute is given by the site potential of mean force (PMF), which is calculated using equation 4 as the natural logarithm of the 1D projection of $g_\gamma(\mathbf{r})$:

$$W_\gamma(r) = -k_B T \ln g_\gamma(r) \quad (4)$$

The lateral loading (or concentration profile) of a solvent, $g_\gamma^{\text{lateral}}(z)$, in a slice with a volume of $\Delta V = xy\Delta z$, where x and y are the unit cell dimensions parallel to the kaolinite plane and the slab thickness in a direction perpendicular to the kaolinite surface Δz , set to 0.25 Å, is calculated by integration of $g_\gamma(\mathbf{r})$ within ΔV as shown in equation 5. The integrated loading of the solvent (or solvation number), $g_\gamma^{\text{integr}}(z)$, for a slab with thickness z is calculated using equation 6.

$$g_\gamma^{\text{lateral}}(z) = \int_{\Delta V(z)} d\mathbf{r} g_\gamma(\mathbf{r}); \quad \Delta V = L_x L_y \Delta z \quad (5)$$

$$g_\gamma^{\text{integr}}(z) = \int_{\Delta V(0)}^{V(z)} d\mathbf{r} g_\gamma(\mathbf{r}); \quad \Delta V(z) = L_x L_y z \quad (6)$$

Before the 3D-RISM-KH calculation, the site-site susceptibility $\chi_{z\gamma}(\mathbf{r})$ between the α and γ sites that enumerate all of the bulk solvent sites is calculated using the dielectrically consistent RISM theory (Perkyns and Pettitt, 1992a, 1992b) and is coupled with the KH closure (DRISM-KH). Dielectrically consistent RISM theory coupled with the KH closure (DRISM-KH) is first used and defined here. It is the reference interaction site model for the solvent. Thorough descriptions of the 3D-RISM-KH molecular theory of solvation have been presented elsewhere (Kovalenko and Hirata, 2000a, 2000b; Kovalenko, 2003; Silveira *et al.*, 2013).

Computational procedure. The DRISM-KH calculations were performed in order to obtain the solvent-solvent susceptibility at 298 K with the density and dielectric constants taken from experimental measurements. The DRISM-KH equations were made discrete and converged to a uniform grid of 8192 points with a spatial resolution of 0.1 Å, which is a grid density that has been shown to be reliable (Silveira *et al.*, 2015). The solvent model of benzene (Jorgensen *et al.*, 1996; Kobryn and Kovalenko, 2008) was based on the all-atom optimized potentials for liquid simulations (OPLS) force field. The 8-site OPLS model was used for toluene (Jorgensen *et al.*, 1993). For the rest of the solvents, the united atom OPLS force field (Jorgensen *et al.*, 1988) was employed using solvent parameters taken from Kobryn and Kovalenko (2008). The solvent input structures and

force field parameters are available in Table S1 (available in the Supplemental Materials section, deposited with the Editor-in-Chief and available at <http://www.clays.org/JOURNAL/JournalDeposits.html>). The site-site susceptibility of the bulk DRISM-KH model solution was used as input for the 3D-RISM-KH integral equation.

The 3D-RISM-KH integral equations 1 and 2 were made discrete on a $64 \times 64 \times 128$ point rectangular grid for a kaolinite sheet that contained $A2 \times B1$ unit cells (2 unit cells along a and 1 unit cell along b , where a and b are along the x and y axes, respectively, as defined in Figure 1, top left) in a $10.298 \text{ \AA} \times 8.934 \text{ \AA} \times 64.00 \text{ \AA}$ model cell filled with a solvent at 298 K. In this system, the parallel images of the kaolinite layer were separated by about 56 Å of solvent, which eliminated kaolinite-kaolinite interactions. The unit cell and structure of kaolinite were taken from the X-ray crystallography of Bish (1993). Non-bonding parameters and partial charges for the kaolinite atoms were obtained from the CLAYFF general force field (Cygan *et al.*, 2004). The image charge effects that arise from the Ewald summation were subtracted numerically to exclude interactions between adjacent kaolinite lamellae. The solvation free energy was calculated analytically from the total and direct distribution functions using equation 3. The kaolinite solute input structure and force field parameters are available in Table S2 (Supplementary Materials section).

RESULTS AND DISCUSSION

Aliphatic (pentane and heptane), cyclic aliphatic (cyclopentane and cyclohexane), and aromatic (benzene and toluene) solvents and a polar solvent (ethanol) were investigated with respect to solvent interactions with kaolinite, which is an abundant clay mineral in the oil sands. The model employed represented site-specific as well as plane-averaged lateral adsorption interactions of the solvents with the hydrophobic siloxane and hydrophilic AlOH surfaces of kaolinite.

Model of kaolinite in solution. The kaolinite model system contained periodically extended platelets isolated by solvent as shown in the solvent box (Figure 1, top). The methylene site density distribution function $g_{\text{CH}_2}(\mathbf{r})$ of cyclopentane, which is the best bitumen extraction solvent because it is highly efficient and has a low boiling point (Wu and Dabros, 2012), is shown as a blue (dark gray in grayscale) isosurface in Figure 1 with an isovalue of 1.1. The 1D projection of the distribution function is along a vector that passes through an axial AlOH group H atom and is perpendicular to the AlOH surface. The vector is shown as a brown (gray in grayscale) dashed arrow that passes through the center of the model kaolinite platelet (Figure 1, top). The 1D projection of $g_{\text{CH}_2}(\mathbf{r})$ is shown as a solid black line (Figure 1, bottom). The surface hydroxyl

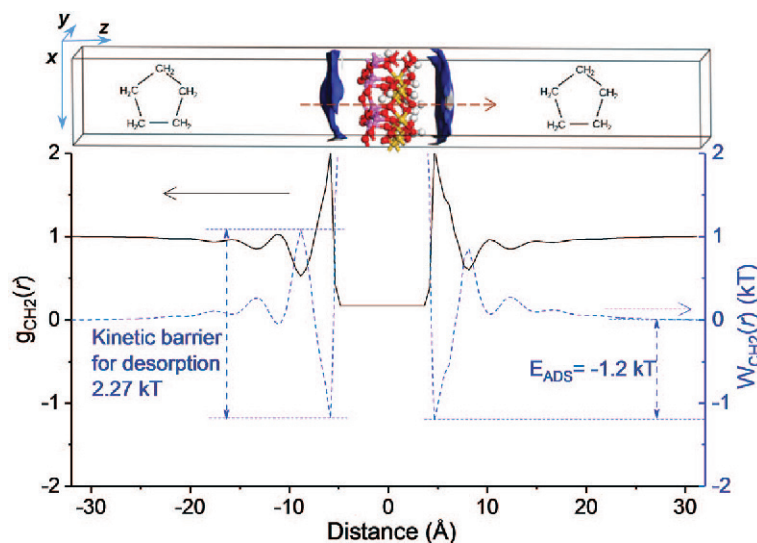


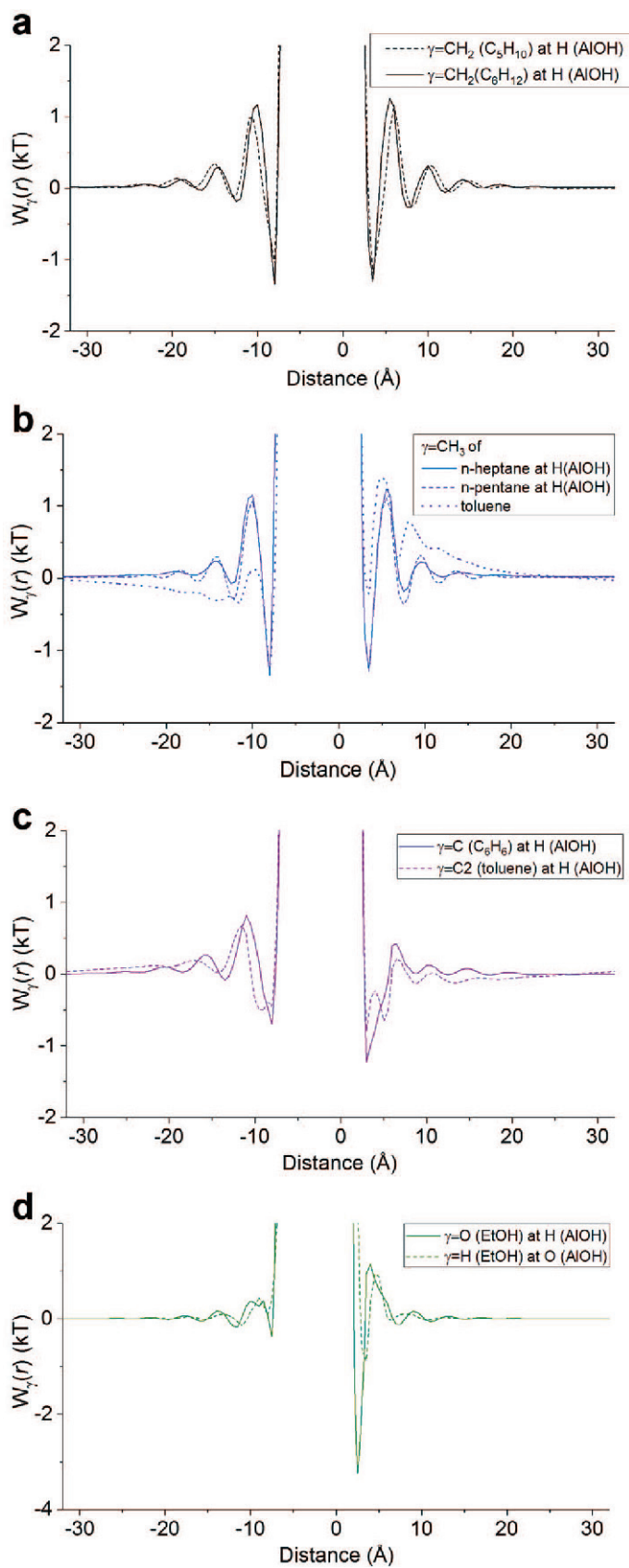
Figure 1. Computational model for the interaction of cyclopentane solvent with a kaolinite platelet. Top: kaolinite platelet immersed in cyclopentane with x , y , and z axes. The isosurface of $g_{\text{CH}_2}(r) = 1.1$ is plotted in blue (dark gray in grayscale). Each methylene group is represented by a single site. The 1D projection vector that passes through an axial OH group H atom of the kaolinite Al-OH surface is shown as a brown (gray in grayscale) dashed arrow; Bottom: 1D projection of $g_{\text{CH}_2}(r)$ along the projection vector (solid black line and left axis label) and the corresponding $W_{\text{CH}_2}(r)$ value, which was calculated using equation 4. In the $W_{\text{CH}_2}(r)$ plot (dashed blue (gray in grayscale) line and right-hand side axis), the energy minimum is labeled as the adsorption free energy E_{ADS} and the $E_{\text{Max-Min}}$ is the kinetic barrier for desorption.

group site was selected because it is a prominent surface feature and a major hydrogen bonding site. The 1D projection has maxima near the two clay platelet surfaces that correspond to the first solvation shells and the lower peaks correspond to the second and subsequent solvation shells. At longer distances from the platelet surface, the distribution function values approach unity, which correspond to the bulk solvent distribution. The 1D projection was near zero in the -5 to $+5$ Å range because the platelet was centered within the cell. The methylene site PMF values, $W_{\text{CH}_2}(r)$, were calculated using equation 4 and are shown by the dashed blue line. Two important solvent-kaolinite interaction characteristics are highlighted at the bottom of Figure 1. The adsorption free energy E_{ADS} was defined as the absolute minimum PMF value and indicated that adsorption to AlOH surfaces was slightly stronger than to SiO surfaces. The relative height of the maximum PMF relative to the minimum PMF is the kinetic barrier for desorption. The desorption barrier on kaolinite SiO surfaces was higher than on AlOH surfaces. Because the value of the desorption barrier was >2 kT, the SiO oxide surfaces would be wetted by a solvent.

Potential of mean force. The PMFs of representative solvent sites allowed a comparison of the solvent-

kaolinite interactions (Figure 2). The results showed that cyclohexane interacted with kaolinite more than cyclopentane (Figure 2a). Also, the n -heptane interacted more strongly than n -pentane, the interaction with toluene was comparable to heptane, and all were evaluated with respect to the methyl group (CH_3) site. The CH_3 sites of these solvents more strongly interacted with the hydrophobic kaolinite SiO surfaces and the barrier heights and depths were comparable to the methylene group (CH_2) sites of the cyclic aliphatic solvents (Figures 2a, 2b). The benzene C sites interacted more strongly with kaolinite surface H atoms than with the SiO surfaces (Figure 2c). The toluene aromatic C2 sites adjacent to the toluene tertiary C atom highlight a distinct behavior that features two preferred positions indicated by the two comparable depth H atom minima for kaolinite AlOH surfaces (Figure 2b). This was due to the proximity of the toluene methyl group which altered the adsorption configuration of toluene in comparison to benzene (Figures 2b, 2c). The strongest solvent-kaolinite interactions occurred between ethanol O atom sites and kaolinite AlOH surface H atoms due to hydrogen bonds formed between ethanol and kaolinite (Figure 2d). The kaolinite AlOH surfaces were solvated by ethanol. Hydrogen-bonding molecules have been shown to

Figure 2 (facing page). Site potentials of mean force $W_{\gamma}(r)$ were calculated using equation 4 and show the adsorption energies and desorption barriers in Figure 1 for (a) the methylene groups of cyclopentane and cyclohexane; (b) the methyl groups of heptane, pentane, and toluene; (c) the aromatic Cs of toluene and benzene; and (d) the H and O of ethanol. The 1D projections are along a vector perpendicular to the surface that contains an H atom, except in (d), where the vector contains the O of AlOH.



preferentially adsorb to kaolinite AIOH surfaces (Fafard *et al.*, 2013) and lead to the formation of hydrogen bonding networks that are indicative of molecular recognition interactions (Huang *et al.*, 2014).

The solvation free energies, $\mu_{\text{solv}}^{\text{KH}}$, were calculated using equation 3 (Table 1). The lower the free energy, the more strongly that kaolinite particles are stabilized in solution. The interaction strength of solvents increased in the order aliphatic to aromatic to cyclic aliphatic, which is in qualitative agreement with the most effective non-aqueous extraction order for hydrocarbon solvents (Wu and Dabros, 2012; Nikakhtari *et al.*, 2013). The solvation free energy of kaolinite in ethanol was substantially lower than in the hydrocarbon solvents due to the strong hydrogen bonding between ethanol and kaolinite AIOH surfaces. Ethanol was tested as cosolvent to enhance the solvation strength of liquid and supercritical CO₂ solvents (Rudyk *et al.*, 2013). The 3D-RISM-KH molecular theory of solvation was selected for the present study because it yields solvation free energies that are analytically calculated from distribution functions computed using adequate statistical sampling.

In Table 1, the E_{ADS} and $E_{\text{Max-Min}}$ values of the PMF on both kaolinite surfaces are also listed for the solvents investigated. The lower and higher E_{ADS} and $E_{\text{Max-Min}}$ values are highlighted in boldface to indicate the solvent adsorption free energy and desorption barrier values. These values indicate the kaolinite surfaces that more strongly interacted with the solvents. Aliphatic and cyclic aliphatic solvents as well as the toluene methyl group had comparable interaction strengths for the two kaolinite surfaces, but adsorption was slightly stronger on the hydrophobic SiO surfaces as would be expected for nonpolar solvents. The aromatic C atoms of benzene interacted more strongly with the H of the AIOH surfaces. The strongest interaction of -3.23 kT was for the ethanol O sites due to hydrogen bonding. The desorption barrier values for both kaolinite surfaces,

$E_{\text{Max-Min}}$, indicated the amount of energy needed to remove the solvent from the surface. For most solvents, higher barriers were computed for desorption from the kaolinite AIOH surfaces due to the localized interactions. The desorption barriers were higher than the adsorption energies because of monolayer solvent organization in the solute surface (Stoyanov *et al.*, 2011). The kinetic barrier for removal of ethanol from the kaolinite surface was as high as 4.37 kT, which indicates a very strong ethanol-kaolinite solvation interaction. The enthalpies of desorption can be determined using desorption thermodynamics analysis, which was shown for heterocyclic compounds in hydrocarbon solvents (Fafard *et al.*, 2013; Huang *et al.*, 2014).

The distribution function maxima were good descriptors of the strongest localized interactions, such as hydrogen bonds. The hydrophobic dispersion interactions were diffuse over large areas of space and difficult to evaluate using 1D projections of $g(\mathbf{r})$ due to a diffuse character. Thus, the lateral distribution functions defined in equation 5 were integrated over slabs around the kaolinite surface and analyzed. Moreover, the integrated distribution functions (equation 6) correlated with the mono- and multi-layer loading of heterocyclic compounds on kaolinite surfaces in solution, which was shown using Brunauer–Emmett–Teller (BET) and Freundlich adsorption isotherms (Fafard *et al.*, 2013; Huang *et al.*, 2014).

Adsorption layers. The lateral and integrated density distributions were shown for slabs with a thickness of 0.5 Å according to equation 5 (where $\Delta z = 0.5$ Å) and equation 6 (Figure 3). The lateral density plots were visually similar to the methylene and methyl site PMF values (Figures 2a, 2b), but highlight important differences between the aromatic C and hydroxyl group sites (Figures 2c, 2d). Unlike the PMF maxima, which were higher for benzene, the lateral distribution functions of the toluene and benzene aromatic C atom sites were very

Table 1. Solvation free energy, $\mu_{\text{solv}}^{\text{KH}}$, and the minima and maxima-minima (in kT) of $W_{\gamma}(r)$ of solvent site γ plotted along a vector that passes through an axial OH group H atom (except the $\gamma = \text{H}$ of ethanol, where the vector contains the axial OH group O) at the kaolinite Al-OH surface, perpendicular to the kaolinite surface (Figure 1). The adsorption free energy E_{ADS} and kinetic barrier for desorption that correspond to the absolute minimum and maximum $W_{\gamma}(r)$ values, respectively, are highlighted in boldface.

Solvent	$\mu_{\text{solv}}^{\text{KH}}$	Site γ	E_{Min} SiO	E_{Min} AIO	$E_{\text{Max-Min}}$ SiO	$E_{\text{Max-Min}}$ AIO
Cyclo-C ₅ H ₁₀	-1.23	CH ₂	-1.19	-1.19	2.27	2.05
Cyclo-C ₆ H ₁₂	1.57	CH ₂	-1.35	-1.30	2.52	2.56
<i>n</i> -C ₅ H ₁₂	3.40	CH ₃	-1.32	-1.27	2.39	2.39
<i>n</i> -C ₇ H ₁₆	3.20	CH ₃	-1.34	-1.27	2.49	2.51
Toluene	3.10	CH ₃	-1.34	-0.23	1.46	1.62
Toluene	-	C2	-0.50	-0.79	1.18	1.01
C ₆ H ₆	2.23	C	-0.69	-1.22	1.50	1.64
EtOH	-33.54	O	-0.37	-3.23	0.75	4.37
EtOH	-	H	0.08	-0.89	0.36	1.81

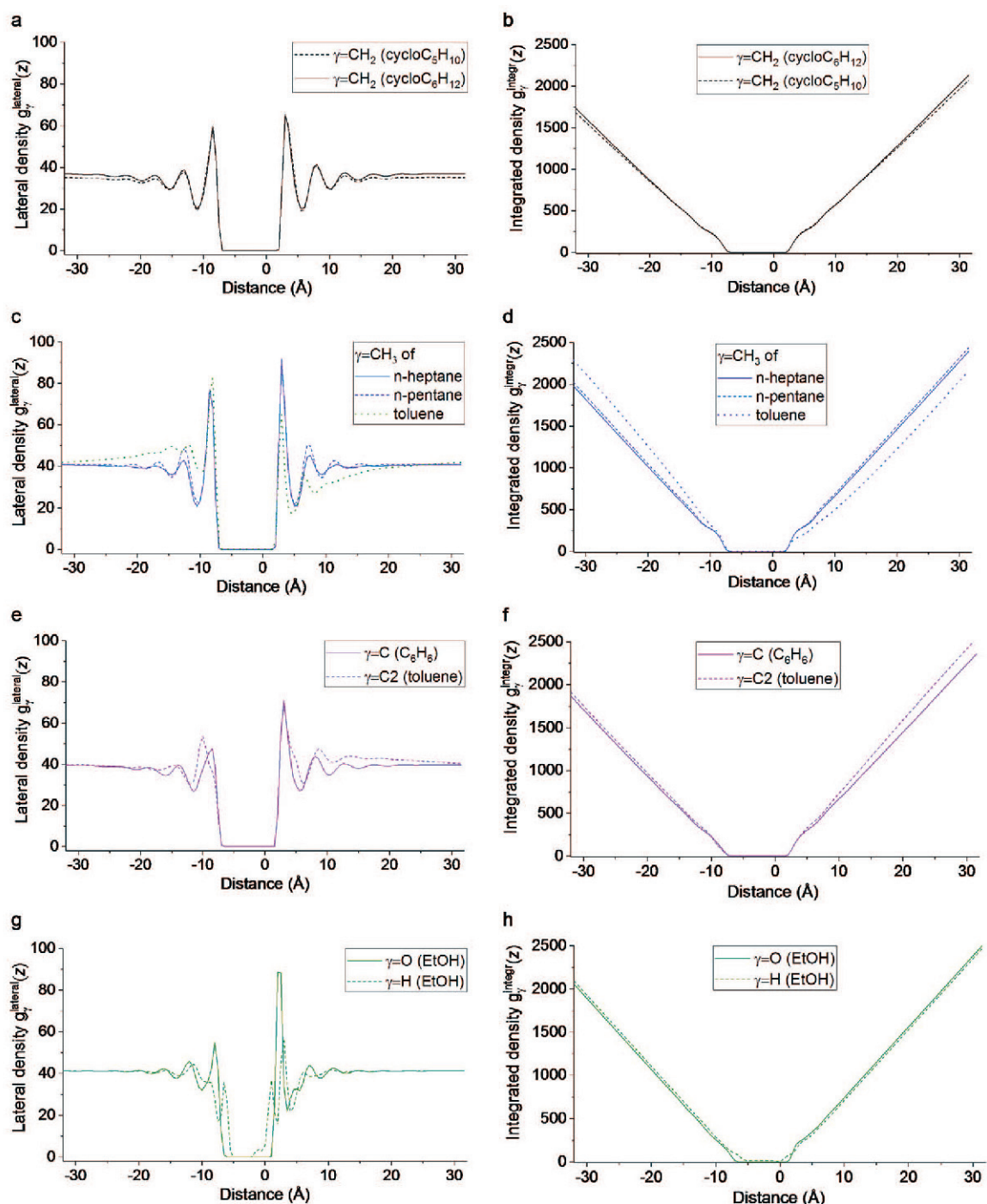


Figure 3. Lateral and integrated density distributions of the methylene groups of cyclopentane and cyclohexane (a and b); the methyl groups of heptane, pentane, and toluene (c and d); aromatic C of toluene and benzene (e and f); and the H and O of ethanol (g and h) around a kaolinite platelet that were calculated using equations 5 and 6.

similar. The adsorption of toluene was greater to both kaolinite surfaces and was indicated by the broader peaks for both kaolinite surfaces. The bulkier shape of toluene produced the difference and reflected the broader first solvation shells for both kaolinite surfaces

in comparison to benzene. The lateral densities for the ethanol hydroxyl sites were also different in that the O sites are farther away from the kaolinite surfaces than the H sites. On the AlOH surfaces, the O sites (the most prominent peak) were farther away than the H sites

because the axial kaolinite hydroxyl groups point away from the surface. At the SiO surfaces, the ethanol H sites are closest to the surface because the exposed O atoms give the entire surface a partial negative charge.

The integrated density distribution plots give a physical meaning to the adsorbent loading curves. The steepest decrease between -10 \AA and $+10 \text{ \AA}$ indicated adsorbed molecules, which correspond to the solvation shells in the lateral density plots (Figure 3). At greater distances from kaolinite particle surfaces, the decreases are less steep and indicate molecules in bulk solution, which correspond to the flat lines in the lateral density plots (Figure 3). Thus, the integrated density plots in proximity of the adsorbent surfaces can be correlated with adsorption isotherms, which was previously demonstrated for heterocyclic compounds in solution (Fafard *et al.*, 2013; Huang *et al.*, 2014).

CONCLUSIONS

Non-aqueous extraction could provide an environmentally acceptable alternative to the currently used warm water process for the recovery of bitumen from oil sands. The main challenge to the large-scale implementation of non-aqueous extraction, *i.e.* recovery of solvent from the tailings after extraction, still requires extensive investigation in order to identify solutions to improve the process.

The 3D-RISM-KH molecular theory of solvation was employed to investigate solvent interactions with kaolinite for both the SiO and AlOH surfaces. The decrease in the order of solvation free energy was correlated to the effectiveness of the hydrocarbon solvents for non-aqueous extraction and highlighted ethanol-kaolinite interactions as the strongest of the investigated solvents. Nonpolar solvents adsorbed to both kaolinite surfaces with comparable strengths if localized interactions were considered, but the hydrophobic SiO surfaces were preferred. Hydroxylated solvents, such as ethanol, form a network of hydrogen bonds with kaolinite AlOH surfaces. The results suggest that solvent removal could be enhanced by using hydroxylated compounds, such as modified cellulose, that could compete with bitumen and solvent for the clay surfaces (Detellier *et al.*, 2015).

The computational results evaluated the solvent-kaolinite interactions that contribute substantially to the retention of solvent in tailings after non-aqueous extraction of bitumen from oil sand. The contributions of other minerals as well as the role of residual bitumen adsorbed to clays and other mineral surfaces to solvent retention in tailings also need further investigation.

ACKNOWLEDGMENTS

The authors acknowledge support from the Government of Canada's interdepartmental Program of Energy Research and Development (PERD) project: Review of Technology Status and Retention of Diluted Bitumen in

Solids. S.R. Stoyanov thanks Dr. John M. Villegas for discussions. The WestGrid-Compute/Calcul Canada national advanced computing platform and CanmetENERGY in Devon computing resources have been utilized for this research. S.R. Stoyanov is Adjunct Professor at the Department of Chemical and Materials Engineering, University of Alberta.

REFERENCES

- Allen, B.L. and Hajek, B.F. (1989) Mineral occurrence in soil environments. pp. 233–236 in: *Minerals in Soil Environments* (J.B. Dixon and S.B. Weed, editors). Soil Science Society of America, Madison, Wisconsin, USA.
- Bensebaa, F., Kotlyar, L.S., Sparks, B.D., and Chung, K.H. (2000) Organic coated solids in Athabasca bitumen: Characterization and process implications. *Canadian Journal of Chemical Engineering*, **78**, 610–616.
- Bish, D.L. (1993) Rietveld refinement of the kaolinite structure at 1.5 K. *Clays and Clay Minerals*, **41**, 738–744.
- Bish, D.L. and Johnston, C.T. (1993) Rietveld refinement and Fourier-transform infrared spectroscopic study of the dickite structure at low temperature. *Clays and Clay Minerals*, **41**, 297–304.
- Chandler, D., McCoy, J., and Singer, S. (1986a) Density functional theory of nonuniform polyatomic systems. I. General formulation. *Journal of Chemical Physics*, **85**, 5971–5976.
- Chandler, D., McCoy, J., and Singer, S. (1986b) Density functional theory of nonuniform polyatomic systems. II. Rational closures for integral equations. *Journal of Chemical Physics*, **85**, 5977–5982.
- Costa, L.M., Hayaki, S., Stoyanov, S.R., Gusarov, S., Tan, X., Gray, M.R., Stryker, J.M., Tykwinski, R., Carneiro, J.W.M., Sato, H., Seidl, P.R., and Kovalenko, A. (2012a) 3D-RISM-KH Molecular theory of solvation and density functional theory investigation of the role of water in the aggregation of model asphaltene. *Physical Chemistry Chemical Physics*, **14**, 3922–3934.
- Costa, L.M., Stoyanov, S.R., Gusarov, S., Tan, X., Gray, M.R., Stryker, J.M., Tykwinski, R., Carneiro, J.W.M., Seidl, P.R., and Kovalenko, A. (2012b) Density functional theory investigation of the contributions of π - π stacking and hydrogen-bonding interactions to the aggregation of model asphaltene compounds. *Energy & Fuels*, **26**, 2727–2735.
- Cygan, R.T., Liang, J.-J., and Kalinichev, A.G. (2004) Molecular models of hydroxide, oxyhydroxide, and clay phases and the development of a general force field. *Journal of Physical Chemistry B*, **108**, 1255–1266.
- Detellier, C., Lataief, S., Fafard, J., and Dedzo, G.K. (2015) Desorption of bitumen from clay particles and mature fine tailings. Patent US20150136651A1.
- Eckert, W.F., Masliyah, J.H., Gray, M.R., and Fedorak, M.R. (1996) Prediction of sedimentation and consolidation of fine tails. *AIChE Journal*, **42**, 960–972.
- Fafard, J., Lyubimova, O., Stoyanov, S.R., Dedzo, G.K., Gusarov, S., Kovalenko, A., and Detellier, C. (2013) Adsorption of indole on kaolinite in non-aqueous media: Organoclay preparation, characterization, and investigation by the 3D-RISM-KH molecular theory of solvation. *Journal of Physical Chemistry C*, **117**, 18556–18566.
- Hansen, J.-P. and McDonald, I.R. (2006) *Theory of Simple Liquids* 3rd ed., Elsevier/Academic Press, London, UK.
- Heaviside, O. (1885) XXX. Electromagnetic induction and its propagation, *The Electrician*.
- Heaviside, O. (1886) XXXY. Electromagnetic induction and its propagation, *The Electrician*.
- Heaviside, O. (1887) XXXVI. Some notes on the theory of the telephone, and on hysteresis. *The Electrician*.

- Hlushak, S. and Kovalenko, A. (2017) Effective interactions and adsorption of heterocyclic aromatic hydrocarbons in kaolinite organic solutions studied by 3D-RISM-KH molecular theory of solvation. *Journal of Physical Chemistry C*, **121**, 22092–22104
- Hlushak, S., Stoyanov, S.R., and Kovalenko, A. (2016) A 3D-RISM-KH molecular theory of solvation study of the effective stacking interactions of kaolinite nanoparticles in aqueous electrolyte solution containing additives. *Journal of Physical Chemistry C*, **120**, 21344–21357.
- Huang, W.-J., Blinov, N., and Kovalenko, A. (2015) Octanol-water partition coefficient from 3D-RISM-KH molecular theory of solvation with partial molar volume correction. *Journal of Physical Chemistry B*, **119**, 5588–5597.
- Huang, W.-J., Dedzo, G.K., Stoyanov, S.R., Lyubimova, O., Gusarov, S., Singh, S., Lao, H., Kovalenko, A., and Detellier, C. (2014) Molecule-surface recognition between heterocyclic aromatic compounds and kaolinite in toluene investigated by molecular theory of solvation and thermodynamic and kinetic experiments. *Journal of Physical Chemistry C*, **118**, 23821–23834.
- Jorgensen, W.L., Laird, E.R., Nguyen, T.B., and Tirado-Rives, J. (1993) Monte Carlo simulations of pure liquid substituted benzenes with OPLS potential functions. *Journal of Computational Chemistry*, **14**, 206–215.
- Jorgensen, W.L., Maxwell, D.S., and Tirado-Rives, J. (1996) Development and testing of the OPLS all-atom force fields on conformational energetics and properties of organic liquids. *Journal of the American Chemical Society*, **118**, 11225–11236.
- Jorgensen, W.L. and Tirado-Rives, J. (1988) The OPLS potential functions for proteins. Energy minimizations for crystals of cyclic peptides and crambin. *Journal of the American Chemical Society*, **110**, 1657–1666.
- Kobryn, A.E. and Kovalenko, A. (2008) Molecular theory of hydrodynamic boundary conditions in nanofluidics. *Journal of Chemical Physics*, **129**, 134701.
- Kovalenko, A. (2003) Three-dimensional RISM theory for molecular liquids and solid-liquid interfaces. pp. 169–275 in: *Molecular Theory of Solvation* (F. Hirata, editor). Series: Understanding chemical reactivity (P.G. Mezey, editor), vol. **24**, Kluwer Academic Publishers, Dordrecht, The Netherlands.
- Kovalenko, A. and Hirata, F. (2000a) Potentials of mean force of simple ions in ambient aqueous solution. I: Three-dimensional reference interaction site model approach. *Journal of Chemical Physics*, **112**, 10391–10402.
- Kovalenko, A. and Hirata, F. (2000b) Potentials of mean force of simple ions in ambient aqueous solution. II. Solvation structure from the three-dimensional reference interaction site model approach, and comparison with simulations. *Journal of Chemical Physics*, **112**, 10403–10417.
- Kovalenko, A. and Hirata, F. (2001) A replica reference interaction site model theory for a polar molecular liquid sorbed in a disordered microporous material with polar chemical groups. *Journal of Chemical Physics*, **115**, 8620–8633.
- Kovalenko, A., Kobryn, A.E., Gusarov, S., Lyubimova, O., Liu, X., Blinov N., and Yoshida, M. (2012) Molecular theory of solvation for supramolecules and soft matter structures: Application to ligand binding, ion channels, and oligomeric polyelectrolyte gelators. *Soft Matter*, **8**, 1508–1520.
- Lage, M.R., Stoyanov, S.R., Carneiro, J.W.M., Dabros, T., and Kovalenko, A. (2015) Adsorption of bitumen model compounds on kaolinite in liquid and supercritical carbon dioxide solvents: A study by periodic density functional and molecular theory of solvation. *Energy & Fuels*, **29**, 2853–2863.
- Levesque, M., Marry, V., Rotenberg, B., Jeanmairet, G., Vuilleumier, R., and Borgis, D. (2012) Solvation of complex surfaces via molecular density functional theory. *Journal of Chemical Physics*, **137**, 224107.
- Li, X., He, L., Wu, G., Sun, W., Li, H., and Sui, H. (2012) Operational parameters, evaluation methods, and fundamental mechanisms: Aspects of nonaqueous extraction of bitumen from oil sands. *Energy & Fuels*, **26**, 3553–3563.
- Lin, F., Stoyanov, S. R., and Xu, Y. (2017) Recent advances in non-aqueous extraction of bitumen from mineable oil sands: A review. *Organic Processes Research & Development*, **21**, 492–510.
- Masliyah, J.H., Czarnecki, J., and Xu, Z. (2011). *Handbook On Theory and Practice of Bitumen Recovery from Athabasca Oil Sands, Volume I: Theoretical basis*. Canada: Kingsley Knowledge Publishing.
- Morales, J.G., Ruez, J., Yamazaki, T., Motkuri, R.K., Kovalenko A., and Fenniri, H. (2005) Helical rosette nanotubes with tunable stability and hierarchy. *Journal of the American Chemical Society*, **127**, 8307–8309.
- Ni, X. and Choi, P. (2012) Wetting behavior of nanoscale thin films of selected organic compounds and water on model basal surfaces of kaolinite. *Journal of Physical Chemistry C*, **116**, 26275–26283.
- Nikakhtari, H., Vagi, L., Choi, P., Liu, Q., and Gray, M.R. (2013) Solvent screening for non-aqueous extraction of Alberta oil sands. *Canadian Journal of Chemical Engineering*, **91**, 1153–1160.
- Nikakhtari, H., Pal, K., Wolf, S., Choi, P., Liu, Q., and Gray, M.R. (2016) Solvent removal from cyclohexane-extracted oil sands gangue. *Canadian Journal of Chemical Engineering*, **94**, 408–414.
- Osacky, M., Geramian, M., Ivey, D.G., Liu, Q., and Etsell, T.H. (2015) Influence of nonswelling clay minerals (illite, kaolinite, and chlorite) on nonaqueous solvent extraction of bitumen. *Energy & Fuels*, **29**, 4150–4159.
- Painter, P., Williams, P., and Mannebach, E. (2010) Recovery of bitumen from oil or tar sands using ionic liquids. *Energy & Fuels*, **24**, 1094–1098.
- Pal, K., Branco, L.P.N., Heintz, A., Choi, P., Liu, Q., Seidl, P.R., and Gray, M.R. (2015) Performance of solvent mixtures for non-aqueous extraction of Alberta oil sands. *Energy & Fuels*, **29**, 2261–2267.
- Palmer, D.S., Frolov, A.I., Ratkova, E.L., and Fedorov, M.V. (2010) Towards a universal method for calculating hydration free energies: A 3d reference interaction site model with partial molar volume correction. *Journal of Physics: Condensed Matter*, **22**, 492101.
- Perkyns, J.S. and Pettitt, B.M. (1992a) A dielectrically consistent interaction site theory for solvent-electrolyte mixtures. *Chemical Physics Letters*, **190**, 626–630.
- Perkyns, J.S. and Pettitt, B.M. (1992b) Site-site theory for finite concentration saline solutions. *Journal of Chemical Physics*, **97**, 7656–7666.
- Rudyk, S., Husain, S., and Spirov, P. (2013) Supercritical extraction of crude oil by methanol- and ethanol-modified carbon dioxide. *Journal of Supercritical Fluids*, **78**, 63–69.
- Rutkai, G. and Kristóf, T. (2008) Molecular simulation study of intercalation of small molecules in kaolinite. *Chemical Physics Letters*, **462**, 269–274.
- Silveira, R.L., Stoyanov, S.R., Gusarov, S., Skaf, M.S., and Kovalenko, A. (2013) Plant biomass recalcitrance: Effect of hemicellulose composition on nanoscale forces that control cell wall strength. *Journal of the American Chemical Society*, **135**, 19048–19051.
- Silveira, R.L., Stoyanov, S.R., Gusarov, S., Skaf, M.S., and Kovalenko, A. (2015) Supramolecular interactions in secondary plant cell walls: Effect of lignin chemical composition revealed with the molecular theory of solva-

- tion. *Journal of Physical Chemistry Letters*, **6**, 206–211.
- Silveira, R.L., Stoyanov, S.R., Kovalenko, A., and Skaf, M.S. (2016) Cellulose aggregation under hydrothermal pretreatment conditions. *Biomacromolecules*, **17**, 2582–2590.
- Sparks, B.D., Kotlyar, L.S., O'Carroll, J.B., and Chung, K.H. (2003) Athabasca oil sands: Effect of organic coated solids on bitumen recovery and quality. *Journal of Petroleum Science and Engineering*, **39**, 417–430.
- Stoyanov, S.R., Gusarov, S., and Kovalenko, A. (2008) Multiscale modelling of asphaltene disaggregation. *Molecular Simulations*, **34**, 953–960.
- Stoyanov, S.R., Gusarov, S., and Kovalenko, A. (2011) Multiscale modeling of the adsorption interaction between model bitumen compounds and zeolite nanoparticles in gas and liquid phase. Pp. 203–230 in: *Industrial Applications of Molecular Simulations* (M. Meunier, editor); Chapter 14. CRC Press, Taylor and Francis Books, Boca Raton, Florida, USA.
- Tan, X., Fenniri, H., and Gray, M.R. (2009) Water enhances the aggregation of model asphaltenes in solution via hydrogen bonding. *Energy & Fuels*, **23**, 3687–3693.
- Tan, X., Vagi, L., Liu, Q., Choi, P., and Gray, M.R. (2016) Sorption equilibrium and kinetics for cyclohexane, toluene, and water on Athabasca oil sands solids. *Canadian Journal of Chemical Engineering*, **94**, 220–230.
- Tanimura, A., Kovalenko, A., and Hirata, F. (2007) Structure of electrolyte solutions sorbed in carbon nanopores, studied by the Replica RISM Theory. *Langmuir*, **23**, 1507–1517.
- Underwood, T., Erastova, V., and Greenwell, H.C. (2016) Wetting effects and molecular adsorption at hydrated kaolinite clay mineral surfaces. *Journal of Physical Chemistry C*, **120**, 11433–11449.
- Wang, T., Zhang, C., Zhao, R., Zhu, C., Yang, C., and Liu, C. (2014) Solvent extraction of bitumen from oil sands. *Energy & Fuels*, **28**, 2297–2304.
- Wu, J.Y. and Dabros, T. (2012) Process for solvent extraction of bitumen from oil sand. *Energy & Fuels*, **26**, 1002–1008.
- Yamazaki, T., Blinov, N., Wishart, D., and Kovalenko, A. (2008) Hydration effects on the HET-s prion and amyloid- β fibrillous aggregates, studied with three-dimensional molecular theory of solvation. *Biophysical Journal*, **95**, 4540–4548.
- Yoshida, K., Yamaguchi, T., Kovalenko, A., and Hirata, F. (2002) Structure of tert-butyl alcohol–water mixtures studied by the RISM theory. *Journal of Physical Chemistry B*, **106**, 5042–5049.

(Received 3 November 2017; revised 18 April 2018; Ms. 1235; AE: C. Detellier)